

## Squeezing of light by a collection of atoms

J. C. Retamal,<sup>1</sup> C. Saavedra,<sup>2</sup> A. B. Klimov,<sup>3</sup> and S. M. Chumakov<sup>4</sup>

<sup>1</sup>*Departamento de Física, Universidad de Santiago, Casilla 307 correo 2, Santiago, Chile*

<sup>2</sup>*Departamento de Física, Universidad de Concepción, Casilla 4009, Concepción, Chile*

<sup>3</sup>*Departamento de Física, Universidad de Guadalajara, Corregidora 500, 44410, Guadalajara, Jalisco, Mexico*

<sup>4</sup>*Instituto de Investigaciones en Matemáticas Aplicadas y Sisitemas, UNAM, Apartado Postal 139-B, 62191, Cuernavaca, Morelos, Mexico*

(Received 25 July 1995; revised manuscript received 28 June 1996)

We study squeezing in electromagnetic field quadrature components, produced by a collection of  $A$  two-level atoms interacting with a single mode of a strong electromagnetic field. We present analytic results both for short and long interaction times. At short times, squeezing grows with the number of atoms for a given initial number of photons. The maximum squeezing which can be achieved in a strong-field case is 66%. At long interaction times, collective effects increase the quadrature fluctuations, compared to the single-atom case. However, for a given number of atoms  $A$ , any initial pure atomic state exhibits squeezing when the mean photon number of the initial coherent field satisfies the condition  $\bar{n} > (2A)^4$ . At times close to the first revival, strong squeezing can be achieved for special initial atomic conditions. [S1050-2947(97)07703-2]

PACS number(s): 42.50.Dv, 42.50.Fx

### I. INTRODUCTION: THE DICKE MODEL

Usually strong quantum electromagnetic fields are generated by lasers as coherent states, which are ‘‘as classical states as possible.’’ How can a resonant interaction with an atomic system modify a strong coherent field so as to make it more ‘‘quantum’’? One of the specifically quantum properties of the field is squeezing in quadrature components. The simplest example, the Jaynes-Cummings model (JCM) [1,2], shows that a small degree of squeezing can be produced by an interaction with a single two-level atom for short interaction times [3,4] and for weak initial fields. This short-time squeezing can be enhanced by the introduction of an initial atomic coherence [5]. Remarkably, the JCM can provide better squeezing for long interaction times and for strong initial coherent fields [6,7]. In the latter case the squeezing goes to 100% in the large mean-photon-number limit ( $\bar{n} \rightarrow \infty$ ). This strong noise reduction occurs for times around the first revival, which depends on the mean photon number as  $t_R = 2\pi\sqrt{\bar{n}}/g$ . It was argued [6–8] that, even taking into account moderate cavity losses that destroy the revival phenomenon, the squeezing survives for large  $\bar{n}$ . Nevertheless, short interaction times seem to be more attractive from the experimental point of view. This region is close to recent experiments in cavity QED [9–11].

One can expect that a way to enhance squeezing is to consider a collection of resonant atoms simultaneously interacting with the field. In the present paper we will work with the Hamiltonian originally proposed by Dicke [12] (also called the Tavis-Cummings model [13]). It describes the interaction of a collection of identical two-level atoms with a single cavity mode of the field. We restrict ourselves to the lossless case. Making the standard dipole and rotating wave approximations for the atom-field interaction, the Hamiltonian reads as follows ( $\hbar = 1$ ):

$$\hat{H} = \omega \hat{N} + g \hat{V}, \quad \hat{V} = a \hat{S}_+ + a^\dagger \hat{S}_-, \quad \hat{N} = \hat{n} + \hat{S}_z. \quad (1.1)$$

Here  $\omega$  is the resonant frequency for the atoms and the ra-

diation field mode is described by the photon operators  $a^\dagger, a$ ,  $\hat{n} = a^\dagger a$ . The collective atomic operators for  $A$  identical two-level atoms are defined as

$$\hat{S}_{\pm,z} = \sum_{j=1}^A \sigma_{\pm,z}^j. \quad (1.2)$$

They obey the usual  $\text{su}(2)$  commutation relations

$$[\hat{S}_z, \hat{S}_\pm] = \pm \hat{S}_\pm, \quad [\hat{S}_+, \hat{S}_-] = 2\hat{S}_z. \quad (1.3)$$

Let us introduce the bare atomic basis

$$\hat{S}_z |k\rangle_{\text{at}} = (k - A/2) |k\rangle_{\text{at}}, \quad 0 \leq k \leq A, \quad (1.4)$$

where the  $k$  label denotes the number of excited atoms. In the space of symmetrical initial states, the atomic operators form an  $(A+1)$ -dimensional representation of the  $\text{su}(2)$  algebra (corresponding to the energy spin  $A/2$ ). The case of a single resonant atom,  $A=1$ , corresponds to the well-known JCM.

The excitation number operator  $\hat{N}$  is a constant of the motion in the Dicke model. If the initial state belongs to a subspace with a given excitation number  $N$ , the system always evolves within this subspace. Thus it is convenient to introduce the basis

$$|N, k\rangle = |n\rangle_f \otimes |k\rangle_{\text{at}}, \quad N = k + n, \quad 0 \leq k \leq A, \\ \hat{N} |N, k\rangle = (N - A/2) |N, k\rangle, \quad (1.5)$$

where  $|n\rangle_f$  is a number state of the field and  $-A/2$  represents the bottom energy level of the atomic system.

The Dicke model can be analytically studied in at least two limit cases: The first occurs when the number of excitations in the system is much smaller than the number of atoms,  $N \ll A$ . This *weak-field region* has been studied in the set of papers given in [14]. Squeezing in the Dicke model in the weak-field region has been discussed in Refs. [15–18]. The second soluble case corresponds to the strong-field re-

gion, when the initial number of photons is much larger than the number of atoms,  $A \ll N$  [19–23]. Numerical evidence for the existence of squeezing in trilinear optical processes (which is mathematically equivalent to the Dicke model) has been reported in [24].

In this paper we employ an analytic approach to study the squeezing properties in the Dicke model (DM) in the strong-field limit for both long- and short-time regions. This article is organized as follows: In Sec. II squeezing properties at the revival regime (for long interaction times) are studied by using the factorization approximation. This approach enables us to describe the dynamics of an arbitrary initial state in terms of a special set of atomic states (semiclassical states). We show that collective phenomena strongly reduce squeezing (compared to the single-atom case) for bare initial atomic states. In the end of the section we briefly discuss the effect of field dissipation for long interaction times by using a numerical simulation.

To discuss squeezing properties in the short-time region we use a more accurate approach [21], which will be referred to as a “quasilinear approximation.” In Sec. III we outline this approximation for the strong-field region and use it to find the Heisenberg field operators. In Sec. IV the maximum squeezing as a function of the number of atoms and of the field intensities is estimated, and the time instant is found when squeezing occurs. In studying short-time squeezing, we restrict ourselves to the case in which all of the atoms are initially excited (the results for initially nonexcited atoms can be obtained from the symmetry properties of the DM [14,19]). The initial field will always be taken to be in a coherent state (CS) with large photon number  $\bar{n} > A$ .

## II. SQUEEZING IN THE REVIVAL REGIME

Squeezing in the JCM in the revival regime has been discovered by Kuklinski and Madajczyk [6]. This case corresponds to the strong-field region, when the average number of photons in the initially coherent field is large:  $\bar{n} \gg 1$ . Strong noise reduction in one of the field quadrature components was predicted. Rigorous study of field properties in the JCM has been carried out by Woods and Gea-Banacloche [7]. They use the expansion of the initial atomic state in the basis of *semiclassical eigenstates* (i.e., eigenstates of the atomic Hamiltonian in an external classical field). If such an initial atomic state interacts with a strong initially coherent field, the total state of the system remains, to high accuracy, factorized into field and atomic parts [25]. This factorization holds for a long-time range  $gt < \bar{n}$ , which covers the revival regime. The evolution of an arbitrary initial atomic state can be described by a superposition of the factorized states. We shall refer to this approach as the *factorization approximation*. This approach has been further extended to describe a wide class of atomic systems interacting with a strong resonant quantum field [19] (see also [22] and [23]). This method gives a very transparent picture of the dynamics in the strong-field region and naturally explains the structure of the quasiprobability distribution (the  $Q$  function) in the field phase space [23]. Here we use it for studying the DM squeezing properties in the revival regime. In fact, the results of the present section should be considered as a generalization of Ref. [7] to the case of many atoms.

### A. Factorization approximation

We start with the definition of the semiclassical atomic states for the Dicke model [23]. In the classical field limit the field operators become complex numbers:

$$\hat{a} \rightarrow \alpha \equiv \sqrt{\bar{n}} e^{i\phi}, \quad \hat{a}^\dagger \rightarrow \bar{\alpha}, \quad (2.1)$$

and the DM Hamiltonian becomes proportional to the operator

$$H_{cl}(\phi) = (S_+ e^{i\phi} + S_- e^{-i\phi})/2 = H(\hat{a} \rightarrow \alpha)/|\alpha|. \quad (2.2)$$

The Hamiltonian  $H_{cl}(\phi)$  describes a collection of two-level atoms in the presence of an external classical field. The phase  $\phi$  of the classical field is chosen to coincide with the phase of the initial coherent state of the field. Semiclassical atomic states are defined as eigenstates of  $H_{cl}(\phi)$ :

$$H_{cl}(\phi)|\underline{p}(\phi)\rangle = \lambda_p |\underline{p}(\phi)\rangle, \quad |\underline{p}(\phi)\rangle = \exp(i\phi \hat{S}_z) |\underline{p}\rangle. \quad (2.3)$$

The semiclassical state with zero phase,  $|\underline{p}\rangle$ , is defined as

$$2\hat{S}_x |\underline{p}\rangle = \lambda_p |\underline{p}\rangle, \quad \lambda_p = A - 2p, \quad p = 0, 1, \dots, A. \quad (2.4)$$

We denote the components of the eigenvectors of the operator  $\hat{S}_x$  in the bare atomic basis as  $C_p^k = \langle k | \underline{p} \rangle$ , i.e.,  $|\underline{p}\rangle = \sum_k C_p^k |k\rangle$ . These coefficients can easily be found from the usual angular momentum theory (see also [14,26]). For a system of  $A$  two-level atoms, there are  $A+1$  different semiclassical states which form a complete basis in the space of all symmetrical atomic states. In what follows we restrict ourselves to the case  $\phi=0$  that distinguishes the  $x$  direction in field phase space, since, for bare initial atomic states, squeezing appears only in the  $x$  direction.

Now let us assume that the initial field is taken to be in a strong coherent state  $|\alpha\rangle$  and that the atomic system is initially prepared in a semiclassical state. Then the total wave function of the system can be approximately written as a product of its field and atomic parts [19,23]:

$$\begin{aligned} |\Psi(t)\rangle &= |\Phi_p(t)\rangle \otimes |A_p(t)\rangle, \\ |\Phi_p(t)\rangle &= \exp[-igt\lambda_p \sqrt{\bar{n}-A/2+1/2}] |\alpha\rangle, \\ |A_p(t)\rangle &= \exp[-i\tau(\hat{S}_z + A/2)] |\underline{p}\rangle, \end{aligned} \quad (2.5)$$

where

$$\tau = \frac{g\lambda_p}{2\sqrt{\bar{n}_A}} t = \frac{\pi t}{t_R}, \quad \bar{n}_A = \bar{n} - A/2 + 1/2. \quad (2.6)$$

The factorization (2.5) holds for times that are short compared to  $t_0 \sim \bar{n}/g$  with an accuracy in coefficients of order  $O(A/\sqrt{\bar{n}})$ . In the simplest case of a single atom,  $A=1$ , Eqs. (2.5) exactly reproduce the result of Gea-Banacloche for the JCM [25].

The field state  $|\Phi_p(t)\rangle$  appears in the factorized wave function as a response to the interaction with the atomic semiclassical state  $|\underline{p}\rangle$ . In field phase space each factorized state can be described by its  $Q$  function, which has the shape of a single hump revolving around a circle of radius  $\sqrt{\bar{n}}$  with

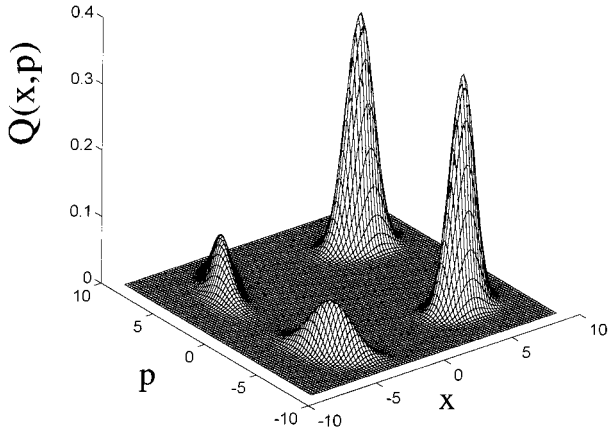


FIG. 1.  $Q$  function of the field at time  $t=t_R/4$  for the three-atom case. All the atoms are assumed to be initially in their excited states. The field is initially taken in a coherent state with  $\bar{n}=49$  and  $A=3$ . The  $Q$  function at this time splits into four humps. All of them are well pronounced as described by Eq. (2.8).

an angular velocity  $g\lambda_p/(2\sqrt{n_A})$  [23]. The photon distribution for these states is always Poissonian, but they spread in phase, due to an intensity-dependent phase shift.

Any initial atomic state can be expanded in the basis of the semiclassical states as

$$|in\rangle_{at} = \sum_p c_p |p\rangle, \quad (2.7)$$

and, correspondingly, the state of a total system can be rewritten as a superposition of the factorized states:

$$|\Psi(t)\rangle = \sum_p c_p |\Phi_p(t)\rangle \otimes |A_p(t)\rangle. \quad (2.8)$$

Hence a generic initial state causes the appearance of  $A+1$  humps which revolve around the circle of radius  $\sqrt{\bar{n}}$  in field phase space with angular velocities  $g\lambda_p/(2\sqrt{n_A})$ . Figure 1 shows the exact  $Q$  function for the field at time  $t=t_R/4$ . We take  $A=3$  and all of the atoms are initially excited. The  $Q$  function of the initial field CS splits into four well-pronounced humps, as we expect from Eq. (2.8). Let us remark in advance that for this time instant each hump exhibits squeezing in some direction. However, the total state is not squeezed, because of the spatial separation of the humps.

The motion of the humps in field phase space determines the behavior of the atomic inversion. When all of the humps are well separated, there are no Rabi oscillations (collapse region). The collision of two humps  $p$  and  $p+1$  leads to the revival of Rabi oscillations (in contrast, the collision of two humps  $p$  and  $p+k$ ,  $k>1$ , does not lead to a revival). The revival time in the Dicke model almost coincides with the JCM revival time [19,23]

$$t_R = 2\pi\sqrt{\bar{n}_A}/g. \quad (2.9)$$

In fact, the representation (2.8) holds exactly for any state of the system (see, e.g., Ref. [22]). What is approximate in Eq. (2.8) are our expressions for the factorized states (2.5). This approximation gives a very transparent qualitative picture of

the dynamics, which will be used below to describe squeezing in the revival regime. However, in the rest of this paper we will need a more accurate approximation, and it will be presented in Sec. III. The derivation of the factorization approximation from the results of Sec. III [and also corrections to the wave functions (2.5)] are given in Appendix C.

### B. Squeezing in factorized states

We start with the case in which the atomic system is prepared in one of its semiclassical states  $|p\rangle$  at  $t=0$ . This leads to the approximate factorization of the wave function. Let us recall that the general quadrature operator is defined as

$$\hat{a}_\theta = (\hat{a}e^{-i\theta} + \hat{a}^\dagger e^{i\theta})/2, \quad (2.10)$$

and a state is said to be squeezed in the  $\theta$  direction if  $\langle\Delta^2\hat{a}_\theta\rangle < 1/4$ . Squeezing in the  $x$  and  $y$  directions correspond to the values  $\theta=\pi$ ,  $2\pi$  and  $\theta=\pi/2$ ,  $3\pi/2$ , respectively.

By reasons which will become clear later, we first calculate the quadrature fluctuations as if the factorization of the wave function were exact. I.e., we first study the noise in the component  $\hat{a}_\theta$  for the pure field states  $|\Phi_p(t)\rangle$  defined by Eq. (2.5). We have

$$\langle\Delta^2\hat{a}_\theta\rangle_p = \langle\Phi_p(t)|\hat{a}_\theta^2|\Phi_p(t)\rangle - \langle\Phi_p(t)|\hat{a}_\theta|\Phi_p(t)\rangle^2. \quad (2.11)$$

Using Eq. (2.5) and making further approximations, it is possible to derive an explicit expression for  $\langle\Delta^2\hat{a}_\theta\rangle$ , as has been done by Kuklinski and Madajczyk [6] for the JCM case. They predicted perfect squeezing in the limit  $\bar{n}\rightarrow\infty$ . For a given value of  $\bar{n}$ , their result works until times  $t\sim\sqrt{\bar{n}}$  Woods and Gea-Banacloche [7] pointed out that squeezing disappears at larger times  $t\sim\bar{n}^{3/4}$ . That is why we wish to present here a better analytical approximation which is valid until times  $gt\sim\bar{n}^{3/4}$ .

It is clear from Eq. (2.5) that the evolution of the field part of the factorized wave function can be described by the following effective Hamiltonian [23]

$$H_{\text{eff}} = g\lambda_p\sqrt{\hat{n}-A/2+1/2}. \quad (2.12)$$

Since we are only interested in terms which remain finite at times  $gt\sim\bar{n}^{3/4}$ , we can approximate the square root in  $H_{\text{eff}}$  as

$$H_{\text{eff}} = g\lambda_p \left[ \sqrt{\bar{n}_A} + \frac{\widehat{\Delta n}}{2\sqrt{\bar{n}_A}} - \frac{(\widehat{\Delta n})^2}{8\bar{n}_A^{3/2}} \right], \quad \widehat{\Delta n} \equiv \hat{n} - \bar{n} \sim \sqrt{\bar{n}}. \quad (2.13)$$

Here we have neglected the term which gives a contribution to the evolution operator of order

$$t \frac{(\widehat{\Delta n})^3}{\bar{n}^{5/2}} \sim \frac{t}{\bar{n}}, \quad (2.14)$$

since this contribution disappears at times  $gt\sim\bar{n}^{3/4}$ . Note that it is senseless to distinguish between  $\bar{n}_A$  and  $\bar{n}$  if they appear in denominators; i.e., we can write  $1/\sqrt{\bar{n}_A} = 1/\sqrt{\bar{n}_A} + O(A/\bar{n}^{3/2})$ . The terms in Eq. (2.5) have a very transparent physical sense: The first term multiplies the wave function by a phase factor (which leads to Rabi oscillations in the case

of bare initial atomic states). The second term rotates the state about the origin of phase space, and the third is responsible for the phase spread.

At this point it is natural to make an analogy to the optical Kerr medium (see, e.g., [27,28]). Indeed, Eq. (2.13) is just the Kerr Hamiltonian. The only difference is the sign of the last term. This difference may be important: E.g., it leads to a strong phase spread reduction when the interactions with the Kerr medium and with the resonant atoms act simultaneously [29]. However, the origin of squeezing in the Kerr medium [27] and in the factorized states of the Dicke model is, in fact, similar. The approximate effective Hamiltonian (2.13) provides an analytic solution for the field Heisenberg operators

$$a(t) = e^{-i\tau} \exp \left[ i\lambda_p g t \left( \frac{1 + 2\widehat{\Delta n}}{8\bar{n}^{3/2}} \right) \right] a. \quad (2.15)$$

Recall that  $\tau = \lambda_p g t / 2\sqrt{\bar{n}}$ . We have, for the mean value of the field operators,

$$\begin{aligned} \langle \hat{a} \rangle_p &= \alpha e^{-i\tau(1-1/4\bar{n})} \exp \left[ \bar{n} \left( e^{-i\tau/2\bar{n}} - 1 + \frac{i\tau}{2\bar{n}} \right) \right] \\ &\approx \alpha e^{-i\tau} e^{-T^2/8}. \end{aligned} \quad (2.16)$$

Thus the phase of the field approximately equals  $-\tau$ , while its amplitude decreases as  $e^{-T^2/8}$  (due to the phase spread); here,  $T = \lambda_p g t / \bar{n}$ . After some algebra, we arrive at the following expression for the quadrature fluctuations:

$$\begin{aligned} \langle \Delta^2 \hat{a}_\theta \rangle_p &\approx \frac{1}{4} + \left[ \frac{\bar{n}}{2} (e^{-T^2/8} - e^{-T^2/16}) + \frac{T}{64} \right. \\ &\quad \left. \times (e^{-T^2/16} - 4e^{-T^2/8}) \right] \cos(2\theta + 2\tau) \\ &\quad + \frac{T\sqrt{\bar{n}}}{8} (2e^{-T^2/8} - e^{-T^2/16}) \sin(2\theta + 2\tau) \\ &\quad + \frac{\bar{n}}{2} (1 - e^{-T^2/16}). \end{aligned} \quad (2.17)$$

For the JCM case,  $\lambda_p = \pm 1$ , one can easily restore the asymptotic result from [6,7]. Replacing  $T = 2\tau/\sqrt{\bar{n}}$  and neglecting all of the terms which contain  $\bar{n}$  in the denominators, one gets

$$\langle \Delta^2 \hat{a}_\theta \rangle_p \approx \frac{1}{4} + \frac{\tau^2}{8} [1 - \cos(2\theta + 2\tau)] + \frac{\tau}{4} \sin(2\theta + 2\tau). \quad (2.18)$$

We show the exact results for the quadrature fluctuation in the  $x$  direction ( $\theta=0$ ) and the approximations (2.17) and (2.18) in Fig. 2. The exact curve (without use of the factorization approximation) and the present approximation (2.17) appear to be very close in this graph, while the asymptotic result (2.18) from Refs. [6,7] shows apparently different behavior for finite photon numbers. Equation (2.17) describes all the essential properties of squeezing under the factoriza-

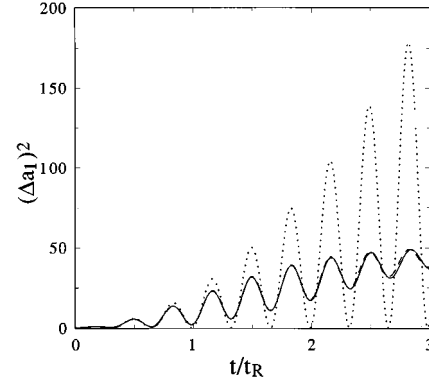


FIG. 2. Squeezing along the  $x$  direction as a function of the normalized time,  $t_n = t/t_R$ , for  $A=3$  and  $\bar{n}=100$ . Atoms are initially prepared in a semiclassical state with  $\lambda_p=1$ . Solid line: exact evolution. Dashed line: analytical approximation, Eq. (2.17). Dotted line: asymptotic approximation, Eq. (2.18). For long interaction times we observe an excellent agreement between the exact evolution and the analytical approximation (2.17). The asymptotic approximation (2.18) fails for long interaction times, for finite values  $\bar{n}$ .

tion approximation. For a given field intensity  $\bar{n}$  and for any chosen direction  $\theta$ , any field state  $|\Phi_p(t)\rangle$  will reveal squeezing at some time instants.

It was noticed in Ref. [7] that squeezing disappears at times  $gt \sim 3\bar{n}^{3/4}$ . One can reproduce this estimation from the following arguments: The phase spread, which initially squeezes the state, at later times deforms it into a crescent shape and causes disappearance of squeezing (see Fig. 1 and the discussion of the  $Q$  function below). The same reason applies to the decreasing of the field amplitude  $|\langle \hat{a} \rangle|$ . In fact, squeezing disappears at times when the field amplitude decreases by unity

$$|\alpha| - |\langle \hat{a} \rangle_p| > 1, \quad (2.19)$$

and we have, from Eq. (2.16),  $\lambda_p g t > \sqrt{8\bar{n}^{3/4}}$ .

We can easily find the direction  $\theta$  in which the maximum squeezing occurs. Differentiating Eq. (2.17) with respect to  $\theta$ , we get

$$\theta_{\max} = -\frac{1}{2} \arccot \left( \frac{\tau}{2} \right) - \tau, \quad (2.20)$$

in full agreement with Ref. [7]. Now it is easy to find the times when squeezing occurs in the  $x$  direction. Replacing  $\theta = k\pi$  ( $k=1,2,\dots$ ) in Eq. (2.20), we get

$$\tau = k\pi - \frac{1}{2} \arccot \left( \frac{\tau}{2} \right). \quad (2.21)$$

The second term is small here, and with reasonable accuracy we can write

$$\tau_{\text{sq}} \equiv \frac{t_{\text{sq}}}{t_R} \pi \approx k\pi - \frac{1}{2} \arccot \left( \frac{k\pi}{2} \right), \quad k=1,2,\dots \quad (2.22)$$

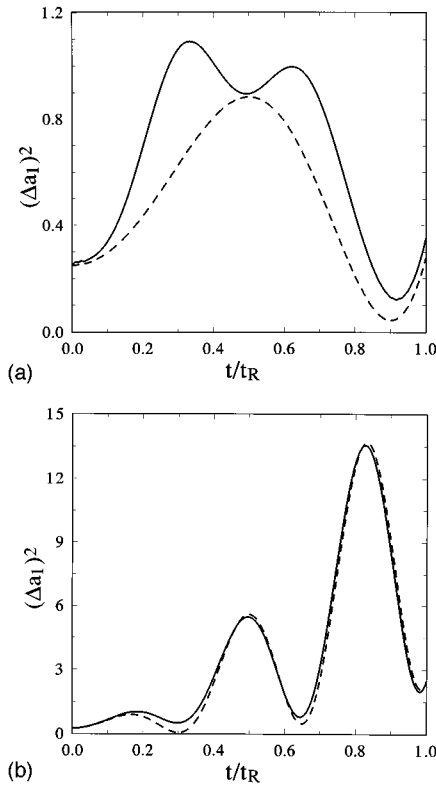


FIG. 3. Squeezing along the  $x$  direction as a function of the normalized time,  $t_n = t/t_R$ , for  $A=3$  and  $\bar{n}=100$ . Atoms are initially prepared in a semiclassical state with (a)  $\lambda_p=1$  and (b)  $\lambda_p=3$ . Solid line: exact evolution. Dashed line: analytical approximation, Eq. (2.17). The time scale for  $\lambda_p=3$  is 3 times the time scale for  $\lambda_p=1$ . In case (b) we observe that squeezing predicted at time  $t_n=1/3$  by the factorization approximation does not occur in the exact evolution. This disagreement arises because of the presence of the secondary humps. The field was initially assumed to be as in Fig. 2.

Hence minimum quadrature fluctuations in the  $x$  direction correspond to times slightly before the revival times:  $t_{sq} \approx 0.9t_R, 1.95t_R, \dots$  [7].

Note that the most important difference between the field parts of the factorized states in the JCM and in the Dicke model occurs in the time scale. In fact, one can write

$$|\Phi_p(t)\rangle \approx |\Phi(\lambda_p t)\rangle, \quad (2.23)$$

where  $|\Phi(t)\rangle$  is the JCM state ( $A=1$ ) with  $\lambda_p=1$ . It can also be seen in the graph of quadrature fluctuations. See Fig. 3, where quadrature fluctuations in the  $x$  direction (exact and under the factorization approximation) are shown for two initial semiclassical states  $p=0$  ( $\lambda_p=3$ ) and  $p=1$  ( $\lambda_p=1$ );  $A=3$  and  $\bar{n}=100$ . For factorized wave functions, the graph for  $\lambda_p=3$  is similar to the 3-times-compressed graph for  $\lambda_p=1$ . This correspondence is less accurate for the exact curves, due to the reason which will be explained below.

The squeezing properties can be naturally explained in terms of the quasiprobability distribution  $Q(\alpha) = |\langle \alpha | \Psi \rangle|^2$  in field phase space. The  $Q$  function corresponding to the state  $|\Phi_p(t)\rangle$  can be represented as follows [23]:

$$Q(\beta = r e^{i\phi})_p = \frac{\exp[-(r-r_0)^2]}{\sqrt{rr_0\mu(t)}} \times \sum_{k=-\infty}^{+\infty} \exp\left[-\frac{(\phi + \phi_0(t) - 2\pi k)^2}{\mu(t)}\right]. \quad (2.24)$$

Here each term is a Gaussian function (of a phase variable) whose center is moving with angular velocity  $\phi_0(t) = tg\lambda_p/(2\sqrt{rr_0} - A/2 + 1/2)$  and with an intensity-dependent variance

$$\mu(t) = \frac{1}{rr_0} + \left(\frac{g\lambda_p t}{2rr_0}\right)^2, \quad r_0 \equiv \sqrt{\bar{n}}, \quad (2.25)$$

which describes a phase spread of the wave packet. Each term in the sum (2.24) contributes for different times. Only the term  $k=0$  is important near the first revival. Then the level curves of the  $Q$  function are given as

$$(r-r_0)^2 + \frac{[\phi - \phi_0(t)]^2}{\mu(t)} = \text{const.} \quad (2.26)$$

These equations confirm the picture which has been described in the previous section: The field state  $|\Phi_p(t)\rangle$  revolves and spreads along the circle of radius  $\sqrt{\bar{n}}$ . For short times  $gt < 3\bar{n}^{-3/4}$ , stretching along the arc of the circle does not differ too much from stretching along a straight line. The level curves of the  $Q$  function are almost ellipses. This has to be expected for squeezed states. But for times  $gt \sim 3\bar{n}^{-3/4}$ , the ellipses are deformed to acquire a crescent shape and the fluctuations of a quadrature component in any direction exceeds 1/4 (the level of fluctuations in a coherent state.)

The predictions of the factorization approximation are rather accurate when they concern the collapses and revivals of Rabi oscillations, the structure of the  $Q$  function, and even the quadrature fluctuations when they are large (see Figs. 1 and 2). Unfortunately, the factorization approximation fails to explain squeezing (or, rather, the absence of squeezing) even in the JCM and, as we now shall see, also in the Dicke model. The question may arise, why do we show the formula (2.17), which does not work? The answer is the following: First, it is still useful under some restrictions. Second, we believe that the field states which enter into the factorized wave functions are important in themselves. They appear for any atomic system interacting with a strong quantum field [19]. Similar field states are produced by the Kerr medium [Eq. (2.17) describes the Kerr medium, if we replace  $T \rightarrow -T$ ].

One should expect from Eq. (2.11) that for  $A > 1$  the best squeezing is reached at times  $t_{sq}/|\lambda_p|$ ,  $p=1, \dots, A$ . For instance, in the case of  $A=3$  we have  $|\lambda_p|=1, 3$ . The  $|\lambda_p|=1$  states revolve with the same angular velocity as in the JCM, and maximum squeezing is expected close to the revival times. In turn, for the states  $|\lambda_p|=3$ , maximum squeezing should appear near the fractional revival time:  $t_{sq}/3$ . Figure 3 tests these predictions against the exact solution for the case of  $A=3$ . We see that the noise reduction at fractional revival times, predicted by the factorization approximation, does not occur in the exact solution. On the other hand, the factorized wave functions still work near the revival times, for both

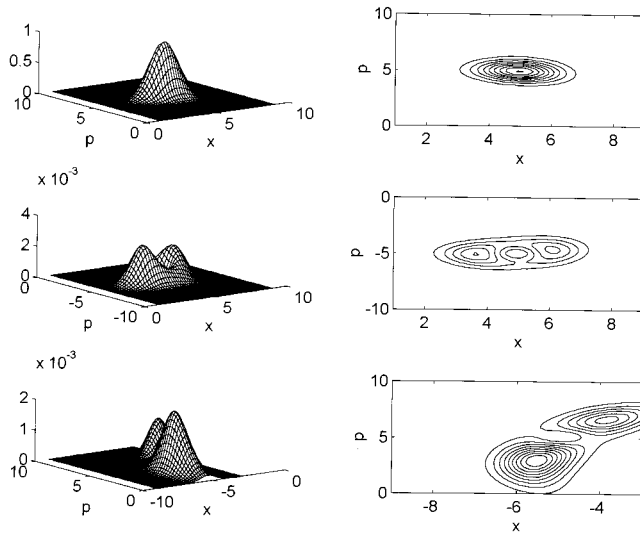


FIG. 4. Exact  $Q$  function of the field at time  $t_n = \frac{1}{4}$  for  $A=3$ ,  $\bar{n}=49$ . Atoms are initially prepared in a semiclassical state with  $\lambda_p=1$ . In order to observe the secondary peak structure, we have split the graph into three pieces, each piece containing a single peak. We emphasize that there is a three-order-of-magnitude difference between the sizes of the main hump and the secondary ones. In principle, there exists another (smaller) hump in the fourth quadrant of phase space, due to the second-order corrections to the factorized wave function.

$\lambda_p=1$  and  $\lambda_p=3$ . As a result, no squeezing appears at fractional revival times. Squeezing can only be expected near the revival times (and only in case it is predicted by the factorization approximation).

In order to explain this behavior, let us consider the exact dynamics of the  $Q$  function in the field phase space, Fig. 4. We notice that, in addition to the well-pronounced hump corresponding to the semiclassical state  $|\Phi_p(t)\rangle$ , there exists some additional structure. This secondary structure consists of small humps which evolve with frequencies,  $g\lambda_q/\sqrt{\bar{n}}$ ,  $q \neq p$ . (The secondary structure in the JCM was discovered in [7].) The heights of additional humps are extremely small compared to the height of the main hill. However, if the secondary humps are far from the main hill, squeezing can be destroyed [7]. Precisely, this happens at fractional revival times; see Fig. 4. At revival time [23] all of the humps get superposed. In this case the field properties are essentially determined by the contribution of the main hump. Then the factorization approximation works and squeezing can appear (see Figs. 3 and 5).

Secondary structure lies beyond the factorization approximation. It can be easily incorporated by considering the corrections to the factorized wave functions (2.5) coming from the contributions of higher powers of the small parameter  $A/\sqrt{\bar{n}}$ . See Appendix C, where it is shown that, at most, two additional humps (associated with the values  $p \pm 1$ ) accompany the main hump  $|\Phi_p(t)\rangle$ . Using the results of Appendix C, a generalization of Eq. (2.11) can easily be found which takes into account the secondary humps. However, it is certainly beyond our present scope of interest. We may only stress that a more accurate description of the dynamical response to the initial atomic semiclassical state leads to a wave function in the form (2.8). This latter equation provides

a general form for an arbitrary initial atomic state. The semiclassical states are distinguished since one of the terms in Eq. (2.8) dominates over the others and the state becomes approximately disentangled.

Generally, squeezing is weaker for the humps which move faster. Indeed, squeezing can only appear at revival times  $2\pi\sqrt{\bar{n}}/g$  independently of the value of  $\lambda_p$ . On the other hand, squeezing cannot be better than predicted by the factorization approximation, Eq. (2.17). As defined by the latter equation,  $\Delta^2\hat{a}$  depends only on  $\lambda_p t$  (not on  $\lambda_p$  and  $t$  separately) and grows when  $\lambda_p g t > \bar{n}$ . For instance, quadrature fluctuations in the states  $|\lambda_p|=3$  (faster humps) are much larger than in the state  $|\lambda_p|=1$  (slow humps), as seen in Fig. 3. For a given semiclassical state, maximum squeezing grows with the field intensity  $\bar{n}$ .

### C. Squeezing for bare initial atomic states

To discuss this item we use the expansion (2.7) of an arbitrary atomic state in the basis of semiclassical states. As mentioned above and shown in Fig. 1, a bare atomic state splits the field  $Q$  function into  $A+1$  humps independently revolving in phase space. Secondary humps are located at the same places as the principal ones and, hence, can be neglected. Strictly speaking, revivals happen when any two humps  $p$  and  $p \pm 1$  collide [23]. However, for the bare initial atomic state it implies that all of the humps get superposed at the revival times. Taking into account the approximate orthogonality of the factorized atomic wave functions at the revival times [19,23] (see also [7]), we obtain the following expression for the quadrature fluctuation of  $\hat{a}_1$  which is valid for times close to revival instants:

$$\langle \Delta^2 \hat{a}_1 \rangle_k = \sum_p |C_k^p|^2 \langle \Phi_p(t) | \hat{a}_1^2 | \Phi_p(t) \rangle - \left( \sum_p |C_k^p|^2 \langle \Phi_p(t) | \hat{a}_1 | \Phi_p(t) \rangle \right)^2. \quad (2.27)$$

Curves produced by making use of this formula are in very good correspondence with the exact results. They show that, for a given initial photon number, squeezing is destroyed very fast with growing numbers of atoms. The physical reasons for the growth of fluctuations are also clear. The structure of the  $Q$  function suggests that squeezing can only occur if all of the humps associated with different semiclassical states coincide in a given region of phase space at the same time. It does happen at the revival times. Thus we can expect squeezing if all of the humps associated with different frequencies  $|\lambda_p|$  are squeezed. On the other hand, we know from the latter section that quadrature fluctuations become much larger for faster humps ( $|\lambda_p| > 1$ ). These fast humps contribute significantly in the dynamics to destroy squeezing for the case of initial bare atomic states. (For a given number of atoms, one can always restore squeezing by means of increasing the initial field intensity.)

We can estimate the ‘‘threshold’’ number of photons for which squeezing appears. The semiclassical state with  $|\lambda_p|=1$  is always squeezed at the first revival time,  $t_R = 2\pi\sqrt{\bar{n}}/g$ . Squeezing is destroyed at times  $\sim 3\bar{n}^{3/4}$ . We may expect squeezing if all of the semiclassical states which con-

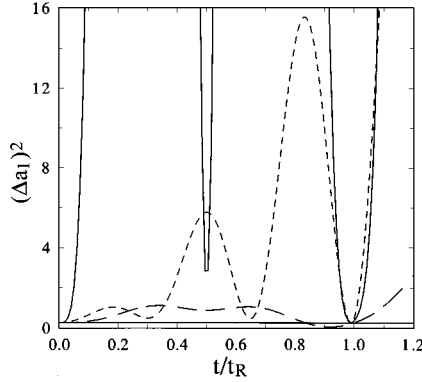


FIG. 5. Threshold for the appearance of squeezing in the revival regime. Squeezing along the  $x$  direction as a function of the normalized time,  $t_n = t/t_R$ , for  $A=3$  and  $\bar{n}=1000$ . Dashed line: semiclassical state  $\lambda_p=1$ . Dotted line: semiclassical state  $\lambda_p=3$ . Solid line: bare atomic state  $|k=3\rangle$ . All the curves are exact.

tribute to the given initial atomic state are squeezed at the revival time. The state with maximum  $|\lambda_p|=A$  has the maximum fluctuations in this regime. This state evolves with the time scale  $At$ , i.e.,  $A$  times faster than the state with  $|\lambda_p|=1$ . Therefore, the faster state is squeezed at the first revival time if  $At_R < 3\bar{n}^{3/4}$ . Thus we arrive at the condition for the existence of squeezing in the revival regime for a system of  $A$  atoms:

$$\bar{n} > (2A)^4. \quad (2.28)$$

If this inequality holds, squeezing appears for any initial atomic state. Our exact numerical evidences are in accordance with this result. We show the graph for the threshold value of  $\bar{n}$ , when squeezing appear, in Fig. 5. Quadrature fluctuations in the  $x$  direction are shown as a function the normalized time  $t_n \equiv t/t_R$  for the semiclassical states with  $\lambda_p=1$  and 3 and for the bare atomic state with all atoms excited,  $|k=3\rangle$ . All the curves in Fig. 5 are exact;  $A=3$  and  $\bar{n}=1000$ . For larger photon numbers, squeezing becomes stronger.

To conclude this section, we may say that the factorization approximation (2.5) describes, at least qualitatively, the squeezing for long interaction times (the revival regime) in the Dicke model. However, the long-time squeezing is strongly suppressed in this model, with respect to the JCM case. In the rest of this paper we will be concerned with short times. It turns out that the direct application of the factorization approximation (2.5) to study short-time squeezing leads to an error. In fact, it is known [3] that short-time squeezing in the JCM decreases with the growth of the field intensity. Hence one can expect an inverse dependence of short-time squeezing on the field intensity. This means that the asymptotic expansion (2.5), with an error in the coefficients of order  $O(A/\sqrt{\bar{n}})$ , is not reliable in this case.

Another argument is that the short-time squeezing appears essentially due to interference among different semiclassical states, which is absent in the factorization approximation [7]. Indeed, the atomic parts of the factorized wave functions are nearly orthogonal at times  $\sim kt_R$ ,  $k=0,1,\dots$ . Thus matrix elements between different factorized states vanish both at

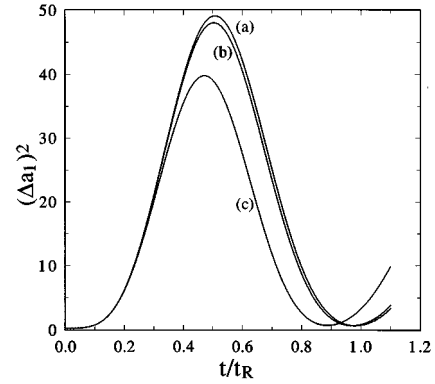


FIG. 6. Effect of field dissipation on the evolution of quadrature fluctuations in the  $x$  direction for two atoms, which are initially prepared in their excited states. The field is taken to be initially in a coherent state with  $\bar{n}=49$ . (a)  $\gamma_c=0$ , (b)  $\gamma_c=10^{-3}$ , and (c)  $\gamma_c=10^{-2}$ . All the curves have been obtained from the exact numerical solution of the dissipative master equation.

short times (until the first collapse) and at revival times. For these reasons we adopt a different scheme to investigate the short-interaction-time region.

#### D. Field dissipation

Up to now, we have considered the system imbedded in an ideal cavity. For short interaction times, around the first collapse  $gt \approx 1$ , the effect of the dissipation can be neglected for the present experimental setup. However, in general, it can be expected that dissipation completely changes the picture for interaction times close to the first revival. Here we include a brief discussion of the field dissipation for typical values of parameters in recent experiments, in which the  $63p_{3/2} \rightarrow 61p_{5/2}$  transition of  $^{85}\text{Rb}$  atoms with a coupling constant  $g=44$  kHz is used and a cavity decay constant  $\gamma_c=2.5$  Hz [30]. Thus we have  $\gamma_c/g \sim 10^{-4}$ . We argue that dissipation should not affect significantly squeezing at times close to the first revival time. For these times squeezing is determined by fluctuations in the semiclassical states which contribute to a given initial atomic condition.

In Fig. 6 we show the effect of dissipation for different values of the field decay constant,  $\gamma_c/g=0, 10^{-3}$ , and  $10^{-2}$ . Even for the worst case  $\gamma_c/g=10^{-2}$ , quadratures fluctuations  $\Delta a_1$  do not increase compared to the non dissipative case (which also means that the dissipation does not affect significantly intensity fluctuations). The main effect of the dissipation appears to be a reduction of the average photon number, which can be approximately given as  $\bar{n}(t) = \bar{n} \exp(-\gamma_c t)$  [31,32]. In fact, the minimum of fluctuations occurs at the revival time; it appears earlier for larger  $\gamma_c/g$ , which corresponds to a decrease of the revival time due to the decrease of the average photon number. Figure 6 also shows that the interference of the semiclassical states around the revival time (small oscillations seen in the curve  $\gamma_c=0$ ) completely disappears for finite values of  $\gamma_c$ . These oscillations are a reminiscence of the revival of Rabi oscillations of the atomic inversion. Recall that dissipation destroys the revival itself for the chosen values of  $\gamma_c/g$ ; i.e., the coherence between the semiclassical states is lost.

Finally, Fig. 6 shows that for chosen values of the decay constant all the curves coincide for short times, as expected,

and the dissipation can be neglected for short times as it will be done in Sec. IV. A more detailed study of the field dissipation in the Dicke model, both analytically and numerically, will be published elsewhere [33].

### III. DM EVOLUTION OPERATOR IN THE QUASILINEAR APPROXIMATION

As we have seen in the previous section, the factorization approximation does not provide enough accuracy to describe squeezing for short times. Better approximations are available [14,21]. We shall use the approximate evolution operator (EO) found in Ref. [21]. (It corresponds to the zeroth-order approximation for the wave functions from Refs. [14], translated to the strong-field region.) In fact, we need to calculate the Heisenberg operators  $a(t)$  and  $a^2(t)$ . However, we include here a brief derivation of the EO for the strong-field case.

Following Ref. [21], let us introduce the transformation

$$\hat{Q} = \exp[i\hat{\phi}(\hat{S}_z + A/2)], \quad (3.1)$$

where  $\exp(\pm i\hat{\phi})$  are the field phase operators [34]. Since the operator  $\hat{S}_z + A/2$  is reduced to integer numbers when acting on the bare atomic states,  $(\hat{S}_z + A/2)|k\rangle_{\text{at}} = k|k\rangle_{\text{at}}$ , the operator  $\hat{Q}$  is a direct sum of different powers of the phase operator:

$$\hat{Q} = \sum_{k=0}^A |k\rangle_{\text{at}} e^{i\hat{\phi}k} \langle k|_{\text{at}}. \quad (3.2)$$

In general  $[\hat{Q}, \hat{Q}^\dagger] = |0\rangle_{\text{ff}} \langle 0|$ . However, acting in the basis (1.5), the  $\hat{Q}$  operator is unitary on the states  $n > A \geq k$ . The following commutation properties of the  $\hat{Q}$  operator will be used later [21]:

$$\begin{aligned} f(\hat{n})\hat{Q}^\dagger &= \hat{Q}^\dagger f(\hat{n} + \hat{S}_z + A/2), & \hat{Q}f(\hat{n}) &= f(\hat{n} + \hat{S}_z + A/2)\hat{Q}, \\ \hat{Q}\hat{S}_+\hat{Q}^\dagger &= \exp(i\hat{\phi})\hat{S}_+, & \hat{Q}\hat{S}_-\hat{Q}^\dagger &= \exp(-i\hat{\phi})\hat{S}_-. \end{aligned} \quad (3.3)$$

Acting on field operators the  $\hat{Q}$  transformation gives

$$\hat{n} \equiv \hat{Q}^\dagger \hat{n} \hat{Q} = \hat{n} - \hat{S}_z - A/2, \quad (3.4)$$

$$\hat{a} \equiv \hat{Q}^\dagger \hat{a} \hat{Q} = \sqrt{\hat{n} - \hat{S}_z - A/2 + 1} e^{i\hat{\phi}} = \sqrt{\frac{\hat{n} - \hat{S}_z - A/2 + 1}{\hat{n} + 1}} \hat{a}. \quad (3.5)$$

Applying the  $\hat{Q}$  transformation to the Dicke Hamiltonian (1.1) and making use of Eqs. (3.3), we diagonalize the Hamiltonian in the field space:

$$\underline{H} \equiv \hat{Q}^\dagger \hat{H} \hat{Q} = g(\sqrt{\hat{n} - A/2 - \hat{S}_z + 1} \hat{S}_+ + \hat{S}_- \sqrt{\hat{n} - A/2 - \hat{S}_z + 1}). \quad (3.6)$$

In the strong-field case, one can expand the transformed Hamiltonian (3.6) in a power series of a small parameter  $(\hat{n} - A/2 + 1/2)^{-1} \ll 1$  (see [21]):

$$\underline{H} = 2g\sqrt{\hat{n} - A/2 + 1/2} \hat{S}_x - \frac{g\{\hat{S}_z, \hat{S}_x\}}{\sqrt{\hat{n} - A/2 + 1/2}} + \dots \quad (3.7)$$

Here  $\{\}$  denotes the anticommutator. It has been shown [21,23,19] that even the zeroth-order approximation (just the first term in the above expansion)

$$\underline{H} \simeq 2g\sqrt{\hat{n} - A/2 + 1/2} \hat{S}_x \quad (3.8)$$

describes well all of the essential quantum phenomena like collapses and revivals of the atomic inversion, trapping states, the wave function factorization, evolution of the  $Q$  function, etc. The EO takes on the form

$$\hat{U}(t) \simeq \hat{Q} \hat{U}_{\text{at}}(t) \hat{Q}^\dagger, \quad (3.9)$$

where

$$U_{\text{at}}(t) = \exp(-i\hat{\tau}\hat{S}_x), \quad \hat{\tau} \equiv 2gt\sqrt{\hat{n} + 1/2 - A/2}. \quad (3.10)$$

This evolution operator has a very simple physical sense. In every subspace with given excitation number  $N$ , it leads to linear dynamics, which is just a precession of the Bloch vector (energy spin  $A/2$ ) around the  $x$  axis. The frequency of this precession (the generalized Rabi frequency),  $\Omega_N = g\sqrt{N - A/2 + 1/2}$ , depends nonlinearly on  $N$ , which accounts for the nonlinearity of the model. We call this a *quasilinear approximation*. For the Jaynes-Cummings case,  $A=1$ , the EO (3.9) reproduces the exact result [all the corrections due to higher order terms in the expansion (3.7) vanish].

The evolution operator (3.9) enables us to easily find all the atomic and field operators in the Heisenberg representation. Since  $[\hat{S}_z, \hat{Q}] = 0$ , the Heisenberg operator  $\hat{S}_z(t)$  is given by

$$\hat{U}_{\text{at}}^\dagger \hat{S}_z \hat{U}_{\text{at}} = \hat{S}_z \cos \hat{\tau} - \hat{S}_y \sin \hat{\tau}. \quad (3.11)$$

In turn, for the photon-number operator we have

$$\hat{n}(t) = \hat{U}^\dagger \hat{n} \hat{U} = \hat{Q} \hat{U}_{\text{at}}^\dagger \hat{Q}^\dagger \hat{n} \hat{Q} \hat{U}_{\text{at}} \hat{Q}^\dagger \equiv \hat{Q} \hat{U}_{\text{at}}^\dagger \hat{n} \hat{U}_{\text{at}} \hat{Q}^\dagger. \quad (3.12)$$

Hence the transformed photon-number operator, Eq. (3.4), evolves with time as

$$\hat{n}(t) \equiv \hat{U}_{\text{at}}^\dagger \hat{n}(t) \hat{U}_{\text{at}} = \hat{n} - A/2 - \hat{S}_z \cos \hat{\tau} + \hat{S}_y \sin \hat{\tau}. \quad (3.13)$$

Making use of the commutation relations for the  $\hat{Q}$  operator, Eqs. (3.3), we finally get

$$\begin{aligned} \hat{n}(t) &= \hat{n} + \hat{S}_z(1 - \cos \hat{\nu}) + \frac{1}{2i} (\hat{S}_+ e^{i\hat{\phi}} \sin \hat{\nu} - \sin \hat{\nu} e^{-i\hat{\phi}} \hat{S}_-) \\ &\equiv \hat{n} + \hat{L}(\hat{n}), \end{aligned} \quad (3.14)$$

where

$$\hat{\nu} = \hat{Q} \hat{\tau} \hat{Q}^\dagger = 2gt\sqrt{\hat{n} + 1/2 + \hat{S}_z}. \quad (3.15)$$

The operator  $\hat{L}(\hat{n})$  in Eq. (3.14) is a function of both atomic and field variables. We only indicate its dependence on the field variables, in order to simplify notations. If initially all the atoms are excited, we have

$$\begin{aligned} \langle A | \hat{n}(t) | A \rangle_{\text{at}} &= \hat{n} + \frac{A}{2} (1 - \cos \hat{\nu}_A), \\ \hat{\nu}_A &\equiv 2gt \sqrt{\hat{n} + 1/2 + A/2}. \end{aligned} \quad (3.16)$$

Similarly, one can get the evolution of the annihilation operator

$$\hat{a}(t) = \sqrt{1 + \hat{n}(t)} \exp(i\hat{\phi}) = \sqrt{1 + \frac{\hat{L}(\hat{n})}{\hat{n}+1}} \hat{a}, \quad (3.17)$$

where  $\hat{L}$  is defined by Eq. (3.14). The evolution of  $\hat{a}^2$  directly follows from the this expression

$$\hat{a}^2(t) = \sqrt{1 + \frac{\hat{L}(\hat{n})}{\hat{n}+1}} \sqrt{1 + \frac{\hat{L}(\hat{n}+1)}{\hat{n}+2}} \hat{a}^2. \quad (3.18)$$

In the strong-field limit ( $\bar{n} \gg A$ ), we can expand the square roots in Eqs. (3.17) and (3.18) in powers of  $1/(\hat{n}+1)$  and take an average over the initial atomic state. Following the standard technique of SU(2) group representation theory (see Appendixes A and B), we calculate the matrix element of the operators  $\hat{a}(t)$  and  $\hat{a}^2(t)$  between the fully excited atomic states:

$$\begin{aligned} \langle A | \hat{a}(t) | A \rangle &= \cos^A \left( \frac{\hat{\nu}_A - \hat{\nu}_{A+1}}{2} \right) \left[ 1 + \frac{AZ_1}{4(\hat{n}+1)} \right. \\ &\quad \left. - \frac{AZ_1(AZ_1+1-Z_1)}{32(\hat{n}+1)^2} \right] \hat{a}, \\ \langle A | \hat{a}^2(t) | A \rangle &= \cos^A \left( \frac{\hat{\nu}_A - \hat{\nu}_{A+2}}{2} \right) \left[ 1 + \frac{AZ_2}{2(\hat{n}+1)} \right. \\ &\quad \left. - \frac{AZ_2}{4(\hat{n}+1)^2} \right] \hat{a}^2, \end{aligned} \quad (3.19)$$

where

$$Z_j = 1 - \frac{\cos[(\hat{\nu}_{A+j} + \hat{\nu}_A)/2]}{\cos[(\hat{\nu}_{A+j} - \hat{\nu}_A)/2]} \quad (3.20)$$

and  $\hat{\nu}_{A+j} = 2gt \sqrt{\hat{n} + j + 1/2 + A/2}$ . The dynamical behavior of the atom-field system is described well by these expressions up to times  $gt \sim \bar{n}$ , with an error in coefficients of order  $O(A/\bar{n})$ .

#### IV. SQUEEZING AT SHORT TIMES

In the short-time regime, we consider only bare initial atomic states. These states split the field  $Q$  function into  $A+1$  humps, which are independently revolving in phase space. Thus the short-time squeezing appears due to the interference between the humps (semiclassical states). For initial bare atomic states, secondary humps overlap with the principal ones and, hence, can be neglected. We will study the quadrature fluctuations for the case of  $\theta=0$  in Eq. (2.10), i.e.,  $\hat{a}_1 = (\hat{a} + \hat{a}^\dagger)/2$ . This choice of  $\theta$  leads to the maximum noise reduction for bare initial atomic states in this regime. Indeed, for each moving hump there always exists a symmetric image with respect to the  $x$  axis, which spreads the  $Q$

function in the  $p$  direction and the minimum fluctuations always occur in the  $x$  direction.

To study the short-time dynamics, we expand Eqs. (3.19) for  $\hat{a}(t)$  and  $\hat{a}^2(t)$  in a power series of a small parameter  $gt/\sqrt{\bar{n}} \ll 1$ . Taking the initial field in a coherent state with zero phase, we get

$$\begin{aligned} \langle \Delta^2 \hat{a}_1 \rangle &= \frac{1}{4} + \frac{\bar{n}}{4} \left\{ A \left[ \frac{1}{\bar{n}} \langle 1 - \cos \hat{\nu}_A \rangle - \left\langle \frac{1 - \cos \hat{\nu}_A}{(\hat{n}+1)} \right\rangle \right] \right. \\ &\quad + \frac{A(gt)^2}{2} \left\langle \frac{1}{(\hat{n}+1)^2} \right\rangle - A \left\langle \frac{(\sin \hat{\nu}_A/2)^4}{(\hat{n}+1)^2} \right\rangle \\ &\quad + A^2 \left[ \frac{(gt)^4}{16} \left\langle \Delta^2 \frac{1}{(\hat{n}+1)} \right\rangle + \frac{1}{4} \left\langle \Delta^2 \frac{(1 - \cos \hat{\nu}_A)}{(\hat{n}+1)} \right\rangle \right. \\ &\quad \left. - \frac{(gt)^2}{4} \left\langle \left\langle \frac{1 - \cos \hat{\nu}_A}{(\hat{n}+1)^2} \right\rangle \right\rangle \right. \\ &\quad \left. - \left\langle \frac{1}{(\hat{n}+1)} \right\rangle \left\langle \frac{1 - \cos \hat{\nu}_A}{(\hat{n}+1)} \right\rangle \right] \right\}, \end{aligned} \quad (4.1)$$

where the average values of the diagonal photon operator  $f(\hat{n})$  in the coherent state  $|\alpha\rangle_f$  are determined as follows:

$$\langle f(\hat{n}) \rangle = \sum_n P_n f(n), \quad \langle \Delta^2 f \rangle = \langle f^2 \rangle - \langle f \rangle^2. \quad (4.2)$$

In the short-time region ( $gt \ll \sqrt{\bar{n}}$ ), all the averages in Eq. (4.1) can be easily calculated. For instance, expanding the shifted arguments of the trigonometric functions in series of  $gt/\sqrt{\bar{n}}$ , we get

$$\left\langle \frac{\cos \hat{\nu}_A}{\bar{n}+1} \right\rangle \approx \frac{1}{\bar{n}} \left[ \langle \cos \hat{\nu}_A \rangle + \frac{gt}{\sqrt{\bar{n}_A}} \langle \sin \hat{\nu}_A \rangle \right].$$

In turn, assuming the Gaussian limit of the Poisson distribution and replacing the sums by corresponding integrals we have

$$\langle \cos \hat{\nu}_A \rangle = \exp \left[ -\frac{g^2 t^2 \bar{n}}{2 \bar{n}_A} \right] \cos(2gt \sqrt{\bar{n}_A}),$$

where  $\bar{n}_A = \bar{n} + 1/2 + A/2$ . After straightforward calculation, keeping terms up to order  $1/\bar{n}$  in Eq. (4.1), we get the following expression for the fluctuations of  $\hat{a}_1$ :

$$\begin{aligned} \langle \Delta^2 \hat{a}_1 \rangle &= \frac{1}{4} + \frac{Agt}{4\sqrt{\bar{n}_A}} \sin(2gt \sqrt{\bar{n}_A}) \exp \left( -\frac{(gt)^2 \bar{n}}{2 \bar{n}_A} \right) \\ &\quad + \frac{A^2}{32\bar{n}} \left[ \exp \left( -2(gt)^2 \frac{\bar{n}}{\bar{n}_A} \right) - \exp \left( -\frac{(gt)^2 \bar{n}}{2 \bar{n}_A} \right) \right] \\ &\quad \times \cos(4gt \sqrt{\bar{n}_A}) + \frac{A^2}{32\bar{n}} (1 - e^{-(gt)^2 \bar{n}/\bar{n}_A}) + O \left( \frac{A^3}{\bar{n}^2} \right). \end{aligned} \quad (4.3)$$

This equation contains all the information about short-time fluctuations in the field quadrature component for different numbers of atoms and different initial field intensities.

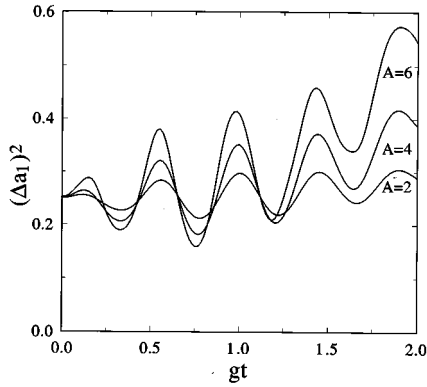


FIG. 7. Short-time squeezing in the  $x$  direction (exact evolution).  $A=2, 4, 6$ . The field is taken to be initially in a coherent state with  $\bar{n}=49$ , and all the atoms initially excited.

Quadrature fluctuations for different numbers of atoms are shown in Fig. 6. For interaction times  $gt \sim 1$ , noise decreases for larger numbers of atoms. When Rabi oscillations collapse the squeezing disappears. (It may appear again around the first revival time.)

In Fig. 7(a) we plot the variance  $\Delta^2 \hat{a}_1$  as a function of time from exact numerical calculation and from Eqs. (3.19), which is valid for long times. We observe a good agreement between curves both for short and medium interaction times. In Fig. 7(b) the same variance is shown for short times; the

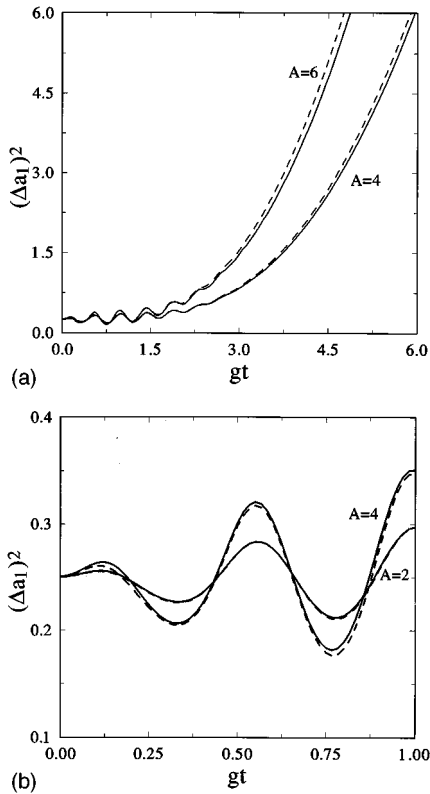


FIG. 8. (a) Short-time squeezing in the  $x$  direction both from the exact evolution (solid line) and from the approximation (3.19) (dashed line);  $A=4$  and  $6$ . (b) Quadrature fluctuations from the exact evolution (solid line) and from the short-time analytic approximation (4.3) (dashed line);  $A=2$  and  $4$ .

exact numerical result is compared with the analytic expression for short times, Eq. (4.3).

Equation (4.3) allows us to find the conditions for the best squeezing and its dependence on the system parameters  $A$  and  $\bar{n}$ . The time instant when the maximum squeezing occurs is determined by the second (secular) term in Eq. (4.3). It describes modulated oscillations. The local maxima of squeezing correspond to the minima of the sine function, which occur at times  $gt(k) = (k-1/4)\pi/\sqrt{\bar{n}_A}$ ,  $k=1,2,\dots$ . The best squeezing occurs at the instant  $t^* = t(k^*)$ , which is the closest to the minimum of the envelope

$$gt_0 = \sqrt{\frac{\bar{n}_A}{\bar{n}}} \sim 1. \quad (4.4)$$

The global minimum is always on the left-hand side of the envelope minimum, as is clearly seen in Figs. 7(a) and 7(b). Precisely, the best squeezing time is given by

$$t^* = \frac{\pi}{g\sqrt{\bar{n}_A}} \left( \left[ \frac{\bar{n}_A}{\pi\sqrt{\bar{n}}} \right] - \frac{1}{4} \right). \quad (4.5)$$

One can arrive at this result by calculating the number of periods of the sine function in the interval  $[0, gt_0]$ . The best squeezing time, to high accuracy, is independent of the number of atoms. However, the maximum squeezing which can be produced in a strong-field region by the system of two-level atoms depends on the number of atoms. Calculating the variance  $\Delta^2 \hat{a}_1$  at the time  $t^*$ , we find

$$(\Delta^2 a_1)_{\text{best}} \approx \frac{1}{4} \left( 1 - a \frac{A}{\sqrt{\bar{n}}} + b \frac{A^2}{8\bar{n}} \right), \quad (4.6)$$

where  $a = e^{-1/2} \approx 0.606$  and  $b = 1 + a - a^2 - a^4 \approx 1.103$ . Squeezing grows linearly with the number of atoms participating in the interaction.

From the above equation one can determine the atomic number which maximizes squeezing for a given mean number of photons in the initial coherent state. We have

$$A_{\text{best}} \sim 2.4\sqrt{\bar{n}}. \quad (4.7)$$

This is consistent with the assumption  $A \ll \bar{n}$  accepted in the quasilinear approximation, provided that  $A/\bar{n} \approx 2.4/\sqrt{\bar{n}} \ll 1$ . If this latter condition is satisfied, one can expect to reach the upper limit for squeezing, which is 66. This is the best squeezing which can be produced in a strong-field region for short interaction times.

For lower field intensities, this theory works for  $A < A_{\text{best}}$ , but not for  $A \sim A_{\text{best}}$  itself. Our numerical tests show that in this case the maximum possible squeezing is less than 66% and that the time instant when the best squeezing occurs moves to shorter times than predicted by Eq. (4.5).

It is worthwhile to note that the small parameter required in the factorization approximation of Sec. II is  $A/\sqrt{\bar{n}} \ll 1$ . The short-time squeezing is proportional to  $A/\sqrt{\bar{n}}$ . Clearly, this effect is beyond the scope of the factorization approximation. In contrast to the long-time squeezing, the short-time one is essentially a consequence of interference between different semiclassical states.

## V. CONCLUSION

We have studied the ability of a collection of resonant two-level atoms interacting with a strong electromagnetic field quantum mode to produce squeezing in the  $\hat{a}_1$  quadrature component. It is assumed that the number of atoms is significantly smaller than the initial number of photons. It is shown that this system exhibits squeezing in both short- and long-time regions.

As in the Jaynes-Cummings model, a significant amount of squeezing can be achieved in the Dicke model at the revival regime if the atomic system is initially prepared in a special state [semiclassical state with the parameter  $\lambda_p = 1$ : see Eq. (2.4)]. Then the noise reduction occurs at an instant slightly before the first revival time. For an arbitrary initial atomic state (e.g., for a bare state), collective effects suppress long-time squeezing, in contrast to the JCM. However, for a given number of atoms, any initial atomic state leads to squeezing, provided that  $\bar{n} > (2A)^4$ .

The fluctuations in the long-time region can be completely analyzed in terms of the factorization approximation, which leads to a very transparent physical picture. However, this approach fails when applied to short times when interference between different semiclassical states is responsible for squeezing.

To study squeezing in the short-time region, we have applied a new operator method developed in [21] which provides better accuracy. In the short-time region, the time instant for best squeezing is almost independent of the number of atoms and is close to the collapse time [see Eq. (4.5)]. The maximum possible squeezing produced by resonant atoms in this region grows with the number of atoms,  $A$ , and is proportional to  $A/\sqrt{\bar{n}}$ . For given  $\bar{n}$ , the best squeezing occurs for  $A \sim 2.4\bar{n}$  and equals to 66%.

The influence of field dissipation on quadrature fluctuations of the field has been numerically studied. For typical values of the parameters in recent experiments,  $\gamma_c/g \sim 10^{-4}$ , we have found that at short times the dissipation can be totally neglected. For long times, the main consequences of dissipation are an exponential decay of the average photon number and a loss of coherence between different semiclassical atomic states, which destroys revivals of Rabi oscillations. However, for moderately high initial photon numbers, dissipation does not significantly affect the squeezing properties of the field. A more detailed study of the effect of dissipation on the Dicke dynamics will be published elsewhere [33].

## ACKNOWLEDGMENTS

We would like to thank P. Minning for carefully reading the manuscript. S. Ch. acknowledges the hospitality of the Departamento de Física, Universidad de Concepción, Chile. This work was supported by Grant No. 1950946, FONDECYT (Chile).

## APPENDIX A

In this appendix we show the details of calculations of the averages  $\langle \hat{a}(t) \rangle$  and  $\langle \hat{a}^2(t) \rangle$ :

$$\hat{a}(t) = U^\dagger(t) a U(t) = \hat{Q} U_{\text{at}}^\dagger(t) \hat{Q}^\dagger a \hat{Q} U_{\text{at}}(t) \hat{Q}^\dagger, \quad (\text{A1})$$

where

$$U_{\text{at}}(t) = \exp(i\hat{\tau} S_x), \quad \hat{\tau}(\hat{n}) = 2gt\sqrt{\hat{n} - A/2 + 1/2}. \quad (\text{A2})$$

We want to calculate the averages over the excited initial atomic state  $|\text{in}\rangle_{\text{at}} = |A\rangle$ . Expanding  $|A\rangle$  in the basis  $|p\rangle$  of eigenvectors of the atomic operator  $S_x$ , Eq. (2.4), we have  $|A\rangle = \sum_p C_p^A |p\rangle$ . The coefficients  $C_p^A = C_n^p$  have been chosen to be real. The expression for the average value over the initial atomic state can be written as

$$\begin{aligned} \langle A | \hat{a}(t) | A \rangle &= e^{i\hat{\phi}A} \langle A | U^\dagger \hat{Q}^\dagger \hat{a} \hat{Q} U | A \rangle e^{-i\hat{\phi}A} \\ &= e^{i\hat{\phi}A} \sum_{p,q} C_p^A C_q^A \langle q | U^\dagger \hat{Q}^\dagger \hat{a} \hat{Q} U | p \rangle e^{-i\hat{\phi}A} \\ &= e^{i\hat{\phi}A} \sum_{p,q} C_p^A C_q^A e^{i\lambda_q \hat{\tau}} \langle q | \hat{Q}^\dagger \hat{a} \hat{Q} | p \rangle e^{-i\lambda_p \hat{\tau}} e^{-i\hat{\phi}A}. \end{aligned} \quad (\text{A3})$$

It still contains the field operators because we have not calculated the average over the initial field state. Introducing the inverse expansion, we have

$$\begin{aligned} \langle A | \hat{a}(t) | A \rangle &= e^{i\hat{\phi}A} \sum_{p,q} C_p^A C_q^A e^{i\lambda_q \hat{\tau}} \sum_{l,k} C_l^q C_k^p e^{-i\hat{\phi}k} \hat{a} e^{i\hat{\phi}l} \\ &\quad \times \delta_{k,l} e^{-i\lambda_p \hat{\tau}} e^{-i\hat{\phi}A}. \end{aligned} \quad (\text{A4})$$

Here we denote  $\hat{\nu}_A = e^{i\hat{\phi}A} \tau e^{-i\hat{\phi}A} = 2gt\sqrt{\hat{n} + A/2 + 1/2}$ . Then

$$\begin{aligned} \langle A | \hat{a}(t) | A \rangle &= \sum_{p,q} C_p^A C_q^A e^{i\lambda_q \hat{\nu}_A} \sum_k C_k^q C_k^p \sqrt{\frac{\hat{n} + 1 - k + A}{\hat{n} + 1}} \\ &\quad \times e^{-i\lambda_p \hat{\nu}_A} \hat{a}. \end{aligned} \quad (\text{A5})$$

We notice that

$$\begin{aligned} \sum_p C_p^A C_k^p e^{-i\lambda_p \hat{\nu}_A} &= \sum_p \langle A | e^{-i\hat{\nu}_A + 1 \hat{S}_x} | p \rangle \langle p | k \rangle \\ &= \langle A | e^{-i\hat{\nu}_A + 1 \hat{S}_x} | k \rangle = d_{Ak}(-\hat{\nu}_A), \end{aligned} \quad (\text{A6})$$

where  $d_{nk}^A(\theta)$  are the usual Wigner  $d$  functions from standard angular momentum theory (see Appendix B). Finally, we get

$$\langle A | \hat{a}(t) | A \rangle = \sum_k d_{Ak}(-\hat{\nu}_A) d_{Ak}(\hat{\nu}_A) \sqrt{\frac{\hat{n} + 1 - k + A}{\hat{n} + 1}} \hat{a}. \quad (\text{A7})$$

In the high-photon-number limit we can expand the square root in the above expression in powers of  $(\hat{n} + 1)^{-1}$ :

$$\begin{aligned} \langle A | \hat{a}(t) | A \rangle &= \sum_{k=0}^A d_{Ak}(-\hat{\nu}_A) d_{Ak}(\hat{\nu}_A) \\ &\quad \times \left( 1 + \frac{A-k}{2(\hat{n}+1)} - \frac{(k-A)^2}{8(\hat{n}+1)^2} \right) \hat{a}. \end{aligned} \quad (\text{A8})$$

Applying formulas from Appendix B, we get Eq. (3.17). Following the same procedure we can obtain the average value of  $\hat{a}^2(t)$ , Eq. (3.18).

### APPENDIX B

Here we outline some properties of Wigner  $d$  functions which are defined as the matrix elements for finite rotations by operators from the SU(2) group representations (see [26]),

$$d_{nk}^A(\theta) = d_{kn}^A(\theta) = \langle k | e^{i\theta \hat{S}_x} | n \rangle, \quad (\text{B1})$$

where  $k, n = 0, 1, \dots, A$ . Here  $A$  is the number of atoms which determines the dimension of the SU(2) group representation,  $\dim = A + 1$ . For example, for the one-atom case ( $A = 1$ ),  $\dim = 2$  and the matrix  $d^1$  is defined as

$$d^A(\theta) = \begin{bmatrix} \cos \frac{\theta}{2} & i \sin \frac{\theta}{2} \\ i \sin \frac{\theta}{2} & \cos \frac{\theta}{2} \end{bmatrix}. \quad (\text{B2})$$

For our calculations we need the functions  $d_{Ak}^A(\theta)$ :

$$d_{Ak}^A = i^{A-k} \sqrt{\frac{A!}{(A-k)!k!}} \sin^{A-k} \frac{\theta}{2} \cos^k \frac{\theta}{2}. \quad (\text{B3})$$

The following sums have been used in calculations [26]:

$$\sum_{k=0}^A d_{Ak}^A(\theta_1) d_{Ak}^A(\theta_2) = \cos^A \frac{(\theta_1 + \theta_2)}{2} \quad (\text{B4})$$

$$\sum_{k=0}^A d_{Ak}^A(\theta_1) d_{Ak}^A(\theta_2) \left( k - \frac{A}{2} \right) = \frac{A}{2} \cos \frac{(\theta_1 - \theta_2)}{2} \times \cos^{A-1} \frac{(\theta_1 + \theta_2)}{2}, \quad (\text{B5})$$

$$\begin{aligned} & \sum_{k=0}^A d_{Ak}^A(\theta_1) d_{Ak}^A(\theta_2) \left( k - \frac{A}{2} \right)^2 \\ &= \frac{A}{4} \cos \frac{(\theta_1 - \theta_2)}{2} \cos^{A-1} \frac{(\theta_1 + \theta_2)}{2} \\ &+ \frac{A(A-1)}{4} \cos^2 \frac{(\theta_1 - \theta_2)}{2} \cos^{A-2} \frac{(\theta_1 + \theta_2)}{2}. \end{aligned} \quad (\text{B6})$$

### APPENDIX C

Here we prove the wave-function factorization used in Sec. II, starting from the evolution operator defined in Sec. III. Applying the  $\hat{Q}^\dagger$  operator to the wave function, we get

$$|\Psi(t)\rangle = \hat{Q} \hat{U} \hat{Q}^\dagger |\text{in}\rangle. \quad (\text{C1})$$

First, we find the action of the  $\hat{Q}^\dagger$  operator on the initial state,

$$|\text{in}\rangle = |\alpha\rangle_f \otimes |p\rangle. \quad (\text{C2})$$

The phase operator acting on the coherent state gives (recall that we take the initial phase to be  $\phi=0$ )

$$e^{\pm i\hat{\phi}k} |\alpha\rangle = |\alpha\rangle + \frac{k\hat{\Delta}n}{2\bar{n}} |\alpha\rangle + O\left(\left[\frac{k}{\sqrt{\bar{n}}}\right]^2\right). \quad (\text{C3})$$

Thus the  $Q$  operator transforms the initial state as

$$\hat{Q}^\dagger |\text{in}\rangle \approx |p\rangle_a \otimes |\alpha\rangle_f - \left[ \frac{\hat{\Delta}n}{2\bar{n}} |\alpha\rangle_f \right] \otimes [(\hat{S}_z + A/2) |p\rangle_a]. \quad (\text{C4})$$

The second term in Eq. (C4) is of order  $O(k/\sqrt{\bar{n}})$ . This term causes the superstructure that destroys squeezing in the factorized states. However, the principal contribution comes from the first term.

Neglecting for a while the influence of the second term, we now let the operator  $\hat{U}$  act on the transformed initial state (C4): From Eqs. (3.8) and (3.9) we have

$$\begin{aligned} \hat{U} |p\rangle_a &= \exp\{-it2g\sqrt{\hat{n}-A/2+1/2}\hat{S}_x\} |p\rangle_a \\ &= \exp\{-it2g\sqrt{\hat{n}-A/2+1/2}\lambda_p\} |p\rangle_a. \end{aligned} \quad (\text{C5})$$

Indeed, since the photon number operator commutes with  $\hat{S}_x, \hat{n}$  can be treated as a  $\mathcal{C}$  number when calculating this exponent. On the other hand,  $|p\rangle_a$  is an eigenvector of  $\hat{S}_x$ . Acting by  $\hat{Q}$  on Eq. (C5) and using the Hermitian conjugate of Eq. (C4), we have

$$|\Psi(t)\rangle \approx \exp\{it2g\lambda_p\sqrt{\hat{n}+\hat{S}_z+1/2}\} |p\rangle_a |\alpha\rangle_f. \quad (\text{C6})$$

The last step is to expand the square root in this expression:

$$\sqrt{\hat{n}+\hat{S}_z+1/2} \approx \sqrt{\hat{n}-A/2+1/2} + \frac{\hat{S}_z+A/2}{2\sqrt{\hat{n}-A/2+1/2}} + O\left(\frac{A^2}{\bar{n}^{3/2}}\right). \quad (\text{C7})$$

These two commuting terms give two commuting factors in the evolution operator, and we have

$$\begin{aligned} |\Psi(t)\rangle &= \exp\{-it2g\lambda_p\sqrt{\hat{n}-A/2+1/2}\} |\alpha\rangle_f \\ &\otimes \exp\left\{\frac{-itg\lambda_p(\hat{S}_z+A/2)}{\sqrt{\hat{n}-A/2+1/2}}\right\} |p\rangle_x. \end{aligned} \quad (\text{C8})$$

This last equation coincides with Eqs. (2.5).

It is also clear how to find the corrections to the factorized wave functions. We need to take into account the second term in Eq. (C4). The evolution operator

$$\hat{U} = \exp\{-it2g\sqrt{\hat{n}-A/2+1/2}\hat{S}_x\}, \quad (\text{C9})$$

acting on the different semiclassical atomic states leads to humps revolving with different angular frequencies, since the atomic operator  $\hat{S}_x$  acting on the semiclassical state  $|p\rangle$  reduces to the number  $\lambda_p$ . Note that  $\hat{U}$  commutes with the photon operator  $\hat{\Delta}n$  in the second term of Eq. (C4). Thus we need to expand the atomic state in the second term of Eq. (C4) in terms of the semiclassical states. This expansion is given as follows:

$$2 \left( \hat{S}_z + \frac{A}{2} \right) |p\rangle = A |p\rangle + \sqrt{(p+1)(A-p)} |p+1\rangle + \sqrt{p(A-p+1)} |p-1\rangle. \quad (\text{C10})$$

Acting on these three terms, the evolution operator  $\hat{U}$  produces three small humps corresponding to  $\lambda_p$  and  $\lambda_{p\pm 1}$ . The hump  $\lambda_p$  is not noticeable since its location coincides with the principal hill, but the humps  $\lambda_{p\pm 1}$  may give a contribu-

tion. Substituting Eq. (C10) into Eq. (C1) and, in turn, substituting it into Eq. (C4), one can get a improved wave function.

This leads to secondary humps discussed in Sec. II. Note that the exact evolution of any state can be presented as a superposition of  $A+1$  factorized states (see, e.g., [22]). However, if a semiclassical atomic state is taken to be an initial atomic state, one of the coefficients in the sum is of order  $\sim 1$ , while the others are of order  $O(A/\sqrt{n})$  or smaller. This is clearly seen in the picture of the  $Q$  function, Fig. 4, where the secondary humps are negligibly small.

- 
- [1] E. T. Jaynes and F. W. Cummings, Proc. IEEE **51**, 89 (1963).  
 [2] B. W. Shore and P. L. Knight, J. Mod. Opt. **40**, 1195 (1993).  
 [3] P. Meystre and M. S. Zubairy, Phys. Lett. A **89**, 390 (1982).  
 [4] P. L. Knight, Phys. Scr. **T12**, 51 (1986).  
 [5] F. X. Zhao, M. Orszag, J. Bergou, and S. Y. Zhu, Phys. Lett. A **137**, 479 (1989).  
 [6] J. R. Kuklinski and J. L. Madajczyk, Phys. Rev. A **37**, 3175 (1988).  
 [7] C. W. Woods and J. Gea-Banacloche, J. Mod. Opt. **40**, 2361 (1993).  
 [8] J. Eiselt and H. Risken, Phys. Rev. A **43**, 346 (1991).  
 [9] H. Walter, Phys. Rep. **219**, 263 (1992).  
 [10] B. J. Hughty, T. R. Gentile, D. Kleppner, and T. W. Ducas, Phys. Rev. A **41**, 6245 (1990).  
 [11] M. Brune *et al.*, Phys. Rev. Lett. **76**, 1800 (1996).  
 [12] R. Dicke, Phys. Rev. **93**, 99 (1954).  
 [13] M. Tavis and F. W. Cummings, Phys. Rev. **170**, 379 (1968).  
 [14] M. Kozierowski, A. A. Mamedov, and S. M. Chumakov, Phys. Rev. A **42**, 1762 (1990); M. Kozierowski, S. M. Chumakov, J. Swiatłowski, and A. A. Mamedov, *ibid.* **46**, 7220 (1992).  
 [15] A. Heidman, J. M. Raimond, and S. Reynaud, Phys. Rev. Lett. **54**, 3226 (1985).  
 [16] M. Butler and P. D. Drummond, Opt. Acta **33**, 1 (1986).  
 [17] M. Kozierowski, A. A. Mamedov, V. I. Man'ko, and S. M. Chumakov, Tr. Fiz. Inst. Akad. Nauk SSSR **200**, 106 (1991).  
 [18] S. S. Hassan, M. S. Abdalla, A.-S. F. Obada, and H. A. Batarfi, J. Mod. Opt. **40**, 1351 (1993).  
 [19] S. M. Chumakov, A. B. Klimov, and J. J. Sanchez-Mondragon, Phys. Rev. A **49**, 4972 (1994).  
 [20] G. Drobny and I. Jex, Opt. Commun. **102**, 141 (1993).  
 [21] A. B. Klimov and S. M. Chumakov, Phys. Lett. A **202**, 145 (1995).  
 [22] P. L. Knight and B. W. Shore, Phys. Rev. A **48**, 642 (1993).  
 [23] S. M. Chumakov, A. B. Klimov, and J. J. Sanchez-Mondragon, Opt. Commun. **118**, 529 (1995).  
 [24] G. Drobny and I. Jex, Phys. Rev. A **46**, 499 (1992).  
 [25] J. Gea-Banacloche, Phys. Rev. A **44**, 5913 (1991).  
 [26] N. Vilenkin and A. Klimyk, *Representation of Lie Group and Special Functions* (Kluwer Academic, Dordrecht, 1991), Vols. 1–3.  
 [27] R. Tanas, in *Coherence and Quantum Optics V*, edited by L. Mandel and E. Wolf (Plenum, New York, 1984), p. 645.  
 [28] G. S. Milburn, Phys. Rev. A **33**, 674 (1986); M. Kitagawa and Y. Yamamoto, *ibid.* **34**, 3974 (1986).  
 [29] S. M. Chumakov, A. B. Klimov, and C. Saavedra, Phys. Rev. A **52**, 3153 (1995).  
 [30] G. Raithel, C. Wagner, H. Walther, L. M. Narducci, and M. O. Scully, in *Cavity Quantum Electrodynamics*, edited by P. R. Gergaman (Academic, New York, 1994), pp. 57–121.  
 [31] J. G. Banacloche, Phys. Rev. A **47**, 2221 (1993).  
 [32] A. B. Klimov, S. M. Chumakov, J. C. Retamal, and C. Saavedra, Phys. Lett. A **211**, 99 (1996).  
 [33] C. Saavedra, A. B. Klimov, S. M. Chumakov, and J. C. Retamal (unpublished).  
 [34] R. Loudon, *The Quantum Theory of Light* (Clarendon, Oxford, 1973), p. 141.